MRI and histologic studies on early markers of Alzheimer's disease

Duijn, S. van

Chapter 2

MRI artifacts in human brain tissue after prolonged formalin storage

Sara van Duijn, MSc* 1, Rob J.A. Nabuurs MD, PhD* 2, Sanneke van Rooden PhD 2, Marion L.C. Maat-Schieman, MD, PhD 3, Sjoerd G. van Duinen MD, PhD 1, Mark A. van Buchem, MD, PhD 2, Louise van der Weerd, PhD 2,4, Remco Natté, MD, PhD 1

* Authors have contributed to this work equally

Departments of Pathology (1), Radiology (2), Neurology (3) and Anatomy & Embryology (4), Leiden University Medical Centre, Leiden, the Netherlands

Mag Reson Med. 2011 June; 65 (6): 1750-1758

Abstract

For the interpretation of magnetic resonance imaging (MRI) abnormalities in brain pathology, often ex vivo tissue is used. The purpose of this study was to determine the pathological substrate of several distinct forms of MR hypointensities that were found in formalin-fixed brain tissue with amyloid-beta deposits. Samples of brain cortex were scanned using effective transverse relaxation time-weighted protocols at several resolutions on a 9.4T MRI scanner. High resolution MRI showed large coarse hypointensities throughout the cortical gray and white matter, corresponding to macroscopic discolourations and microscopic circumscribed areas of granular basophilic neuropil changes, without any further specific tissue reactions or amyloid-beta related pathology. These coarse MRI hypointensities were identified as localized areas of absent neuropil replaced by membrane/myelin sheath remnants using electron microscopy. Interestingly, the presence/absence of these tissue alterations was not related to amyloid deposits, but strongly correlated to the fixation time of the samples in unrefreshed formalin. These findings show that prolonged storaged of formalin fixed brain tissue results in subtle histology artifacts, which show on MRI as hypointensities that on first appearance are indistinguishable from genuine brain pathology. This indicates that postmortem MRI should be interpreted with caution, especially if the history of tissue preservation is not fully known.

Keywords: MRI, ex vivo, formalin

Introduction

Magnetic resonance imaging (MRI) of postmortem brain tissue offers a valuable research method to study disease related changes in image contrast, because the findings can be correlated to histology (1-12). High resolution ex vivo imaging has been a useful tool in interpreting the MRI features of many neurodegenerative disorders, including multiple sclerosis (MS), Alzheimer's disease (AD), and (sporadic) cerebral amyloid angiopathy (1-3, 6-9, 11, 12). However, the MR characteristics of the tissue rapidly change in the postmortem situation because of tissue decomposition and chemical fixation; therefore direct translation of the findings to the clinical setting has to be done with caution (13-19).

First, tissue decomposition occurs during the postmortem interval (PMI), the time period between the patient's somatic death and beginning of the immersion-fixation of the tissue, which varies among subjects. Several studies have shown that an increasing PMI leads to a reduction of T1 and T2 (13, 15, 20). However, a more recent study suggested that these findings might mainly be due to tissue dehydration or the fixative itself. When these effects were minimized, proton density, T1 and T2 values all increased with longer PMI (17). Also, mean diffusivity and fractional anisotropy decrease with prolonged PMI (17, 21).

After autopsy, brain tissue will be immersed into a solution containing a chemical fixative, most frequently being formalin also known as formaldehyde. These solutions preserve tissue by slowly diffusing into it, leading to the cross-linking of proteins and immobilization of water molecules, thereby preventing autolysis and tissue decomposition (21-23). By its nature it is to be expected that this would affect MR characteristics, which indeed was confirmed by several postmortem brain MRI studies. A reverse in gray matter (GM)/white matter (WM) T1 contrast occurs within several days of fixation, merely due to a rapid decline in the latter combined with a general decrease in both continuing at least up to 3 months (18). Similarly, T2 relaxation declines with prolonged fixation affecting both GM and WM, reaching a stable plateau as shown by consecutively imaging up to 6 months fixation (13-15, 18).

All of the above has lead to important considerations on the correct method to obtain and interpret postmortem MR images (13, 15).

However, similar studies investigating the effect of long fixation periods (> 6 months) on the MR characteristics have not yet been published. Nevertheless, this question is important, especially when using rare ma-

Table 1
Subject characteristics and corresponding macroscopic, MRI and histology scores

Subject nr.	Age / Sex (yr)	Post mortem pathologic evaluation	Fixation period (yr)	PMI (hrs)	Macroscopic discoloration	Coarse MR Hypo intensities	Granular neuropil changes
1	88/F	AD	0.3		Absent	Absent	Absent
2	29/M	Control	0.3		Absent	Absent	Absent
3	70/F	sCAA	0.5		Absent	Absent	Absent
4	53/M	Control	0.5		Absent	Absent	Absent
5	53/M	Control	0.5		Absent	Absent	Absent
6	71/M	sCAA	0.5		Absent	Unknown	Absent
7	49/M	DS	1	13	Absent	Absent	Absent
8	64/M	AD	6	48	Present	Present	Present
9	58/M	HCHWA-D	6	6	Present	Present	Present
10	73/M	AD	7	9	Present	Present	Present
11	65/F	AD	7	2	Present	Extensive	Present
12	50/F	HCHWA-D	9	21	Present	Extensive	Extensive
13	45/F	HCHWA-D	15		Present	Extensive	Extensive
14	90/F	AD	16		Present	Extensive	Extensive
15	52/M	HCHWA-D	17	1	Present	Extensive	Extensive
16	62/F	DS	19		Present	Extensive	Extensive
17	62/M	Control	26		Present	Extensive	Extensive
18	58/F	AD	42	14	Present	Extensive	Extensive

M = Male; F = Female; sCAA = sporadic cerebral amyloid angiopathy; DS = Down's syndrome; AD = Alzheimer's disease; HCHWA-D = hereditary cerebral hemorrhage with amyloid Dutch type; PMI = Postmortem interval; MRI coarse hypointensities: Absent = 0; Present = 1 -10 hypointensities in one image; Extensive ≥ 10 hypointensities in at least one of the two examined images. Granular neuropil changes: Absent = 0; Present = 1-4 changes per section; Extensive ≥ 5 changes in at least 1 of the 3 sections.

terial from tissue archives, which are stored using fixatives like formalin for periods ranging from several years to decades. In a recent study using archival tissue with prolonged fixation times, we noticed unusually large coarse hypointensities, especially apparent on high resolution effective transverse relaxation time (T2*) weighted images, in several brain samples regardless of their pathological diagnosis. We hypothesized that these coarse hypointensities were the result of the extended formalin fixation period.

Therefore, the purpose of this study was to investigate the occurrence of these T2* changes with respect to their formalin fixation time in brain samples with different pathologies. To this end, MR images were obtained of 18 samples with fixation times ranging from 3 months to several decades. Subsequently, the samples were evaluated both macroscopically and microscopically to identify the occurrence and the microscopic substrate of tissue changes due to prolonged fixation.

Table 2: Granular neuropil changes of long and short fixed tissue from the same subjects.

Subject	Age / Sex (yr)	Port mortem diagnosis	Granular neuropil changes Fixation period:	
			< 0.5 yr	9 - 42 yr
13	45/F	HCHWA-D	-	+
15	52/M	HCHWA-D	-	+
17	62/M	Control	-	+
18	58/F	AD	-	+

HCHWA-D = Hereditary cerebral hemorrhage with amyloid Dutch type,

AD = Alzheimer's disease

Materials and Methods

Subjects

We used brain tissue of six patients with AD, four patients with Hereditary Cerebral Haemorrhage with Amyloidosis, Dutch type (HCHWA-D), two patients with Down's Syndrome (DS), two patients with sporadic Cerebral Amyloid Angiopathy (CAA) and four control brains (Table 1). The brain tissue had been routinely immersed in buffered 10% formalin for several weeks to 6 months after which the wet tissue was archived in sealed plastic bags with a small excess of 10% formalin. Total fixation times varied from 4 months to 42 years. From a subset of subjects, several samples of the exact same brain had also been paraffin embedded at the beginning of their fixation process, normally within 1 month postmortem. This allowed a direct comparison of structural changes with tissue from the same patients that was archived in formalin and embedded in paraffin several years later (Table 2).

Table 3: pH-measurements

Subject	Post mortem diagnosis	Fixation period (yr)	pH
5	Control	0.5	6.62
12	HCHWA-D	9	6.11
15	HCHWA-D	17	4.98
17	Control	26	5.43
18	AD	42	5.12
Fresh formalin			7

HCHWA-D = Hereditary cerebral hemorrhage with amyloid Dutch type, AD = Alzheimer's disease

Magnetic Resonance Imaging

A slice of 20x15 mm brain tissue was selected from each subject and cut into a 4-mm-thick slice using a vibratome (VT1000S, Leica Microsystems, Wetzlar,

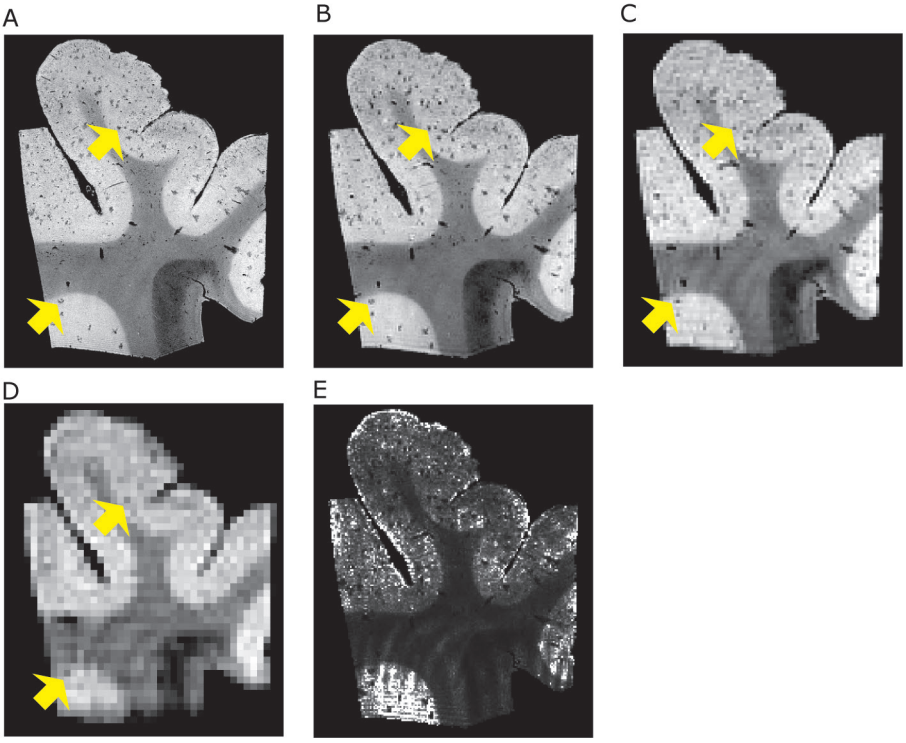

Figure 1: Similar T2* weighted MR images of subject 14 acquired with isotropic resolution of respectively A) 40 µm, B) 100 µm, C) 200 µm and D) 400 µm. Many coarse hypo intensities are detected in the higher resolution, but even in D) hypo intense voxels correlate back to them (white arrows). E) Shows the calculated T2* map of the section in B) with the previously seen hypo intensities having a lower T2* then the surrounding tissue.

Germany). The 4-mm slice was placed in a custom made tissue holder, immersed in a proton-free fluid (Fomblin, Solvay, Solexis, Milan, Italy) and positioned in a vertical small-bore 9.4T Bruker Avance 400WB MRI system, equipped with a 1T/m actively-shielded gradient insert and Paravision 4.0 imaging software (Bruker Biospin, Ettlingen, Germany). A 20-mm birdcage transmit/receive coil was used (Bruker BioSpin). Several three dimensional T2*-weighted gradient echo sequences were obtained with isotropic resolutions of 40 – 100 – 200 – 400 µm with the number of signal averages being 60 – 20 – 20 – 12 respectively, echotime/pulse repetition time = 12.26 / 75 ms, flip angle = 25º. With the matrix size depending on the shape of each sample, average scan time per resolution were 28 hrs, 2 hrs 40 min, 20 min. and 8 min respectively. For quantitative T2* measurements, 100 µm scans were also acquired using echo time = 8 – 10 – 12.26 – 15 ms.

Histology

Following MRI, brain slices were paraffin-embedded and serially cut in 8-µm sections. Consecutive sections were stained for general microscopic morphology (hematoxylin and eosin (HE)), for myelin (Kluver-Barrera), for iron (Perls and a modified Perls DAB) (24), (FEIII-DAB, FEII-DAB) (25), copper (Romeis) and immunohistochemistry for Aβ (Dako, 6F/3D) (26), and glial fibrillary acidic protein (GFAP) (Dako, 6F2) (27). To allow correlation with MRI, sections were digitalized using a flatbed scanner (Agfa).

Electron microscopy

Electron microscopy was performed on a subset of subjects (Table 2) as previously described (28). Collection was done on copper grids instead of carbon grids. Sections were examined using a JEOL JEM-1011 electron microscope operating at 60 kV and digitalized using a MegaView III camera.

Analysis / Scoring

Two sequential MR slices from the three dimensional data sets at 40 um resolution were examined for "coarse" hypointensities defined by large size (120-1200um), irregular contour and elongated to stellate shape. These coarse hypointensities were scored as follows: absent: 0 coarse hypo intensities, present: 1-9 coarse hypointensities, extensive: ≥10

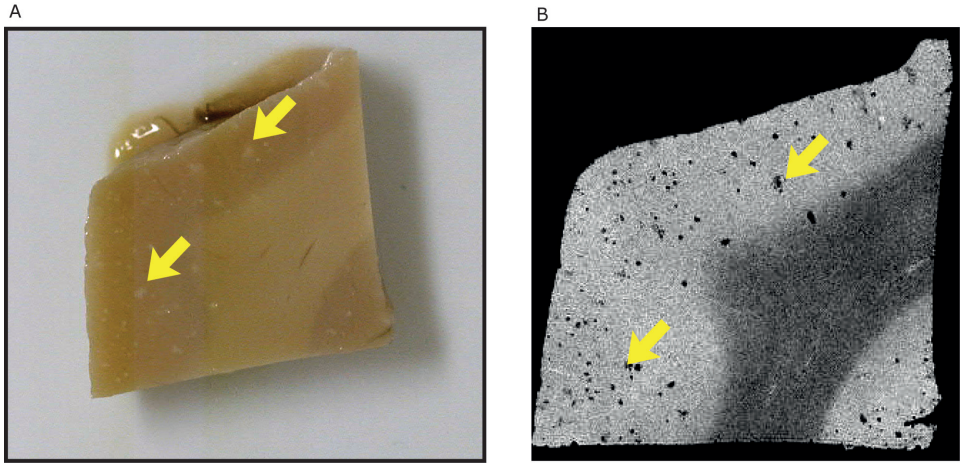

Figure 2: Images from subject 13 showing A) fixated brain tissue with white discolourations (white arrows) and B) high resolution (40µm) T2* weighted MR images of the same brain tissue with coarse hypo intensities (white arrows).

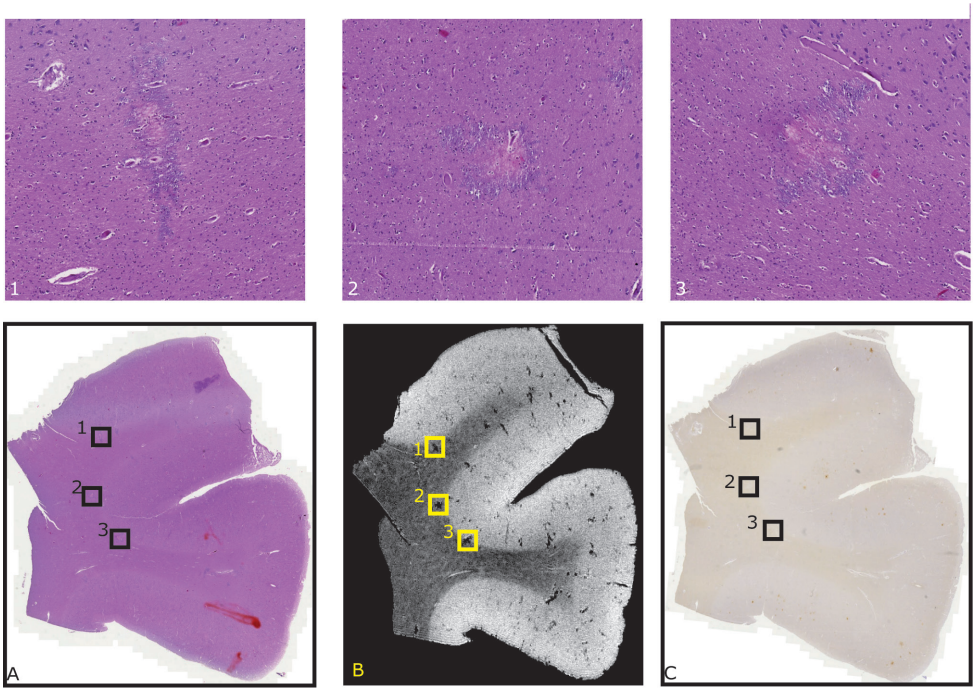

Figure 3: Images of subject 17. Comparison of MR image with HE staining and Aβ staining correlating the granular neuropil changes with the hypointensities in the MRI. The rectangles are the locations of 10x magnifications 1, 2 and 3. Showing that granular neuropil changes can be found at the same location as the hypo intensities but without amyloid deposition. Scale bars are given. A: HE staining; B: MR image; C: Aβ staining

coarse hypointensities. Three HE stained sections from the same level of the two sequential MRI slices were used to correlate MR images with histology. To perform these correlations, we used Adobe Photoshop 6.0 to visually overlay digitalized histological sections to their corresponding MR images. Of each patient, the same HE sections were used to score the amount of granular neuropil changes as follows: absent if no granular neuropil changes were found, present for 1-4 and extensive for ≥ 5 neuropil changes in at least one out of the three sections.
Subjects with similar score were combined for group analysis (Mann-Whitney) to find significant differences (P-value < 0.05) in fixation period and age (SPSS 17).

pH of formalin

Of five patients with widely variable fixation times (Table 3), the pH of the formalin around the brain slices in sealed plastic bags was determined using a logging pH meter (Hanna, H1 98230).

Results

Magnetic resonance imaging

High resolution T2*W images of 11 subjects showed irregularly contoured, elongated and stellate shaped hypointensities that were randomly distributed throughout the cortical gray matter and to a lesser degree in the white matter (Fig.1A). Their typical size (120 – 1200µm) and characteristic shape allowed clear distinction from possible other brain structures known to have a similar effect on T2*, e.g., blood vessels or small roundish hypointensities caused by amyloid-β (Aβ) plaques, especially when including their spatial orientation (Fig.4). Based on these characteristics, we defined them as "coarse hypointensities" and tissue was scored according to their presence (Table 1).

When comparing similar MR images of the same section at decreasing resolution (Fig.1A-D), these coarse hypointensities became less pronounced and harder to recognize as such. This depended on their actual size and shape being affected by partial volume effects due to increasing voxel size. High and low resolution data were compared with assess, if hypointense voxels on low resolution scans correlated with coarse hypointensities at high resolution. The largest coarse hypointensities were also visible at the lowest isotropic resolution of 400 µm, which is comparable to the in vivo MRI resolution (Fig.1D). On quantitative T2* maps, areas containing coarse hypointensities caused a clearly noticeable decrease in T2* (Fig. 1E).

Pathology

Macroscopy

Only in brain tissue with coarse hypointensities on MRI, well circumscribed, white discolourations with similar size and distribution as the coarse MRI hypointensities were observed (Fig. 2, Table 1).

Histology

Microscopically, HE sections of tissue blocks with macroscopic white discolourations showed neuropil alterations with a close spatial correlation to the coarse MRI hypointensities (Fig. 3 and 4). These neuropil alterations comprised irregular, well circumscribed areas of granular, basophilic changes usually with some tissue rarefaction (Fig. 5). The corresponding Kluver's staining within these areas was decreased with respect to sur-

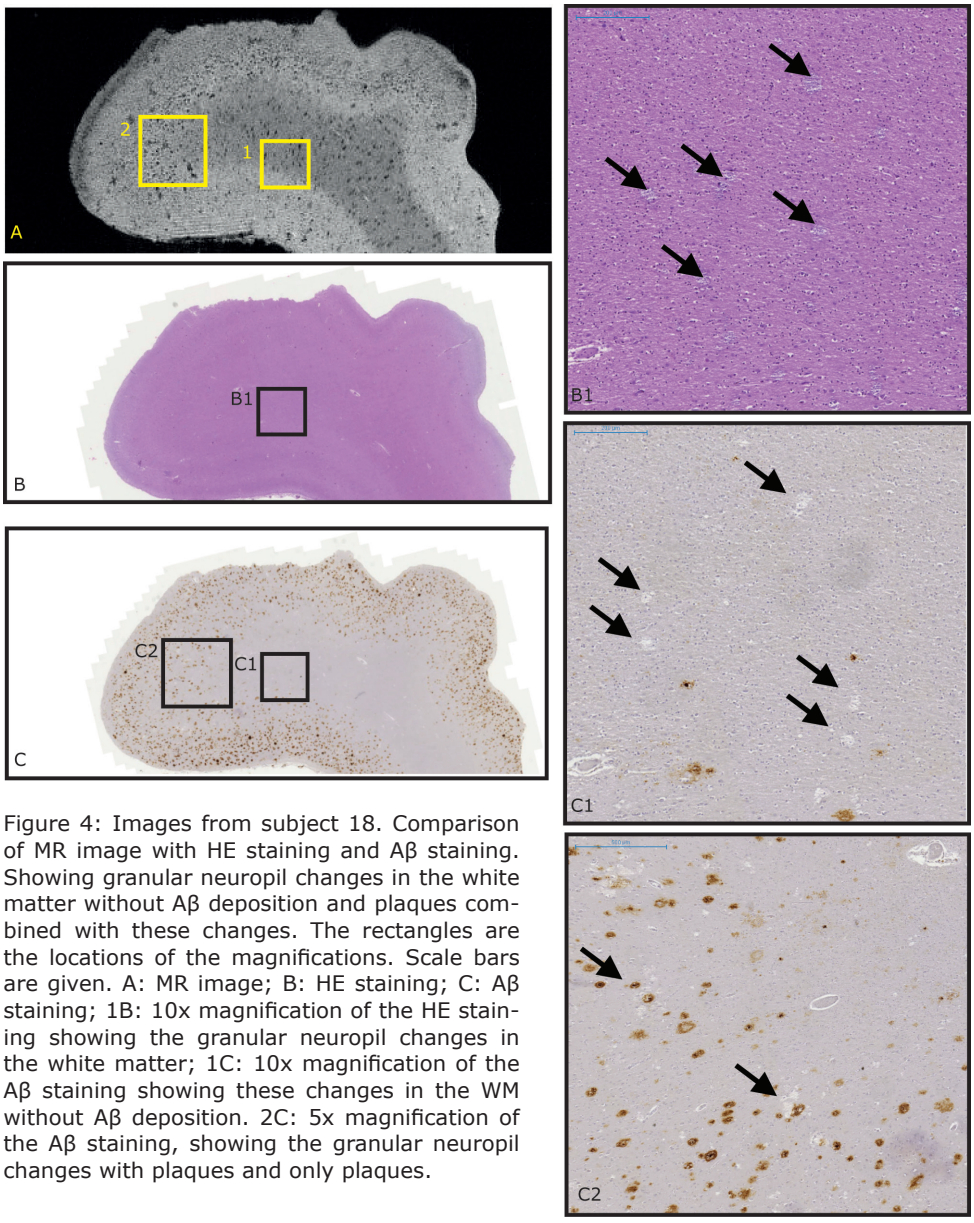

Figure 4: Images from subject 18. Comparison of MR image with HE staining and Aβ staining. Showing granular neuropil changes in the white matter without Aβ deposition and plaques combined with these changes. The rectangles are the locations of the magnifications. Scale bars are given. A: MR image; B: HE staining; C: Aβ staining; 1B: 10x magnification of the HE staining showing the granular neuropil changes in the white matter; 1C: 10x magnification of the Aβ staining showing these changes in the WM without Aβ deposition. 2C: 5x magnification of the Aβ staining, showing the granular neuropil changes with plaques and only plaques.

rounding cortex/white matter suggesting a lower density of myelin. Most of these areas showed birefringence under polarized light in the HE that was not seen in unstained sections or the Kluver's stain that excludes the presence of anorganic material. The areas of basophilic granular neuropil changes were randomly distributed throughout the cortex and increasingly present in the white matter of tissue with long fixation times. These areas were found around vessels but also apart from vessels. The basophilic granular neuropil changes showed no signs of gliosis, haemorrhages or infarcts. Neurons, astrocytes, microglia and vessels were normally distributed within these areas and morphologically unaltered. Gemistocytes were not present. Furthermore, all (immuno) histological stainings for iron, copper and amyloid-β were negative within these areas (Fig. 4). The basophilic granular neuropil changes were found not only in AD material but also in long fixated brain tissue of controls (Fig. 3 and 4). In contrast, these changes were not found in short fixated AD material.
Apart from the coarse hypointensities that co-localized with neuropil degeneration, other small roundish hypointensities were observed on MRI that did correspond to amyloid plaques (Fig. 4).

Electron microscopy

Tissue with macroscopic white discolourations showed localized areas with absent neuropil, although vessels were often present in these spaces on 1 µm -thick, epoxy embedded tissue sections stained with toluidine blue. Electron microscopy of immediately adjacent ultrathin sections showed that these areas with absent neuropil actually consisted of spaces without any neuropil or only little neuropil remnants (Fig. 6A). However, in these spaces varying amounts of lamellar structures were

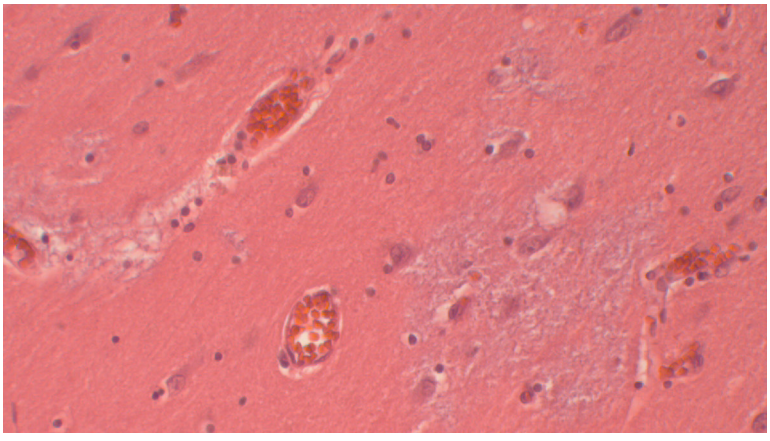

Figure 5: HE 20x Granular neuropil changes

found, which were interpreted as membrane remnants and/or swollen degenerated myelin sheaths (Fig. 6B-C). Outside these circumscribed areas, we observed variable splitting and swelling of myelin sheets ranging from little splitting in otherwise normal myelin sheaths around axons, to swollen myelin sheaths lining small empty spaces within the neuropil (Fig. 6D-E).

Relation of coarse MR hypointensities with fixation duration

The presence of coarse MR hypointensities, macroscopic and microscopic abnormalities were scored for each subject and the results are shown in Table 1. Subjects with similar scores were combined for group analysis.

With regard to coarse MR hypointensities, fixation periods were significantly shorter when scored "absent" compared to "present" (P-value = 0.017 / r = -0.79). Furthermore, with even longer fixation periods, the number of hypointensities significantly increases when comparing "present" with "extensive" (P-value = 0.018 / r = -0.71).

Similar results were obtained when comparing groups with different scores for granular neuropil changes. Fixation periods of those scored "absent" were significantly shorter when compared with those who scored "present" (P-value = 0.006 / r = -0.82), which was significantly shorter as compared to "extensive" cases (P-value = 0.008 / r = -0.80).

No significant differences in subject's age between groups were found for either coarse hypointensity, histological or macroscopic score. Furthermore, no correlation was found between coarse MR hypointensities and presence/absence of disease regardless of type of disease.

In summary, brain tissue showed no changes when fixed for a period of < 1 year in the same formalin solution, whereas changes were always present in tissue fixed for a period of > 6 year, and increasingly so with longer fixation periods.

To test the hypothesis that prolonged formalin fixation indeed leads to histological and MR detectable changes, brain tissue from the same subject that was formalin fixed for either a short or a much longer period was compared microscopically (Table 2). In the long-term fixed material, macroscopic white discolourations and granular neuropil changes were present, whereas short-term fixed material of the same subject completely lacked these findings, indeed supporting our hypothesis.

To obtain a complete picture, pH measurements were performed, because

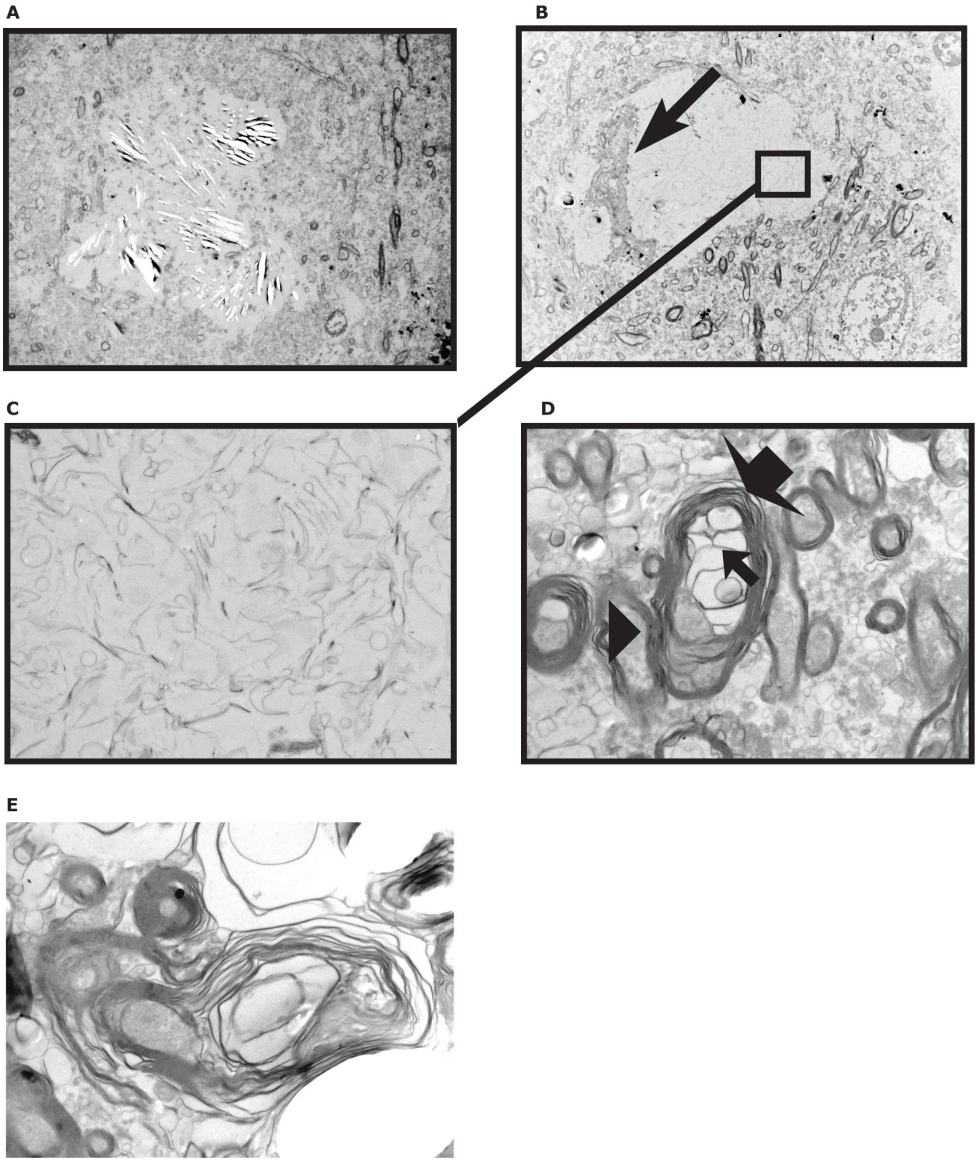

Figure 6: Ultrastructure of localized areas of nearly empty spaces on semithin sections in long term formalin fixed tissue with macroscopic white discolourations. A) These areas consisted of spaces without neuropil or only little neuropil remnants and often but not always contained a small blood vessel (1200X) B) Circumscribed area of absent neuropil showing lamellar structures and a capillary (arrow) (1200X). C) Lamellar structures in B (15000X). D) myelinated axons, some with splitting of the myelin sheath. One axon (arrowhead) shows myelin splitting (large arrow) with little expansion of the spaces between the myelin sheaths (small arrow) (15000X). E) myelinated axon partly with intact myelin sheath and partly with myelin splitting with transition to more laminated structures with increasing spaces between the lamellae.

formalin solutions are known to become more acidic over time. pH measurements indeed showed increased acidity after longer periods of formalin fixation, as observed in the sealed plastic bags used for tissue storage (Table 3).

Discussion and Conclusion

In this study, "coarse hypointensities" on postmortem brain MRI were seen corresponding to localized areas of neuropil destruction with remnants of membranes and myelin sheaths as observed by electron microscopy. These coarse hypointensities are mainly detected at high-resolution MR scans. Although brain tissue from Aβ-related diseases was used, the hypo intensities where not related to deposits of iron, copper or Aβ correlating with these neurological diseases. Instead, these hypointensities appear to be an art1fact associated with the duration of fixation within the same formalin. This can be concluded from the findings that these hypointensities were also detected in control tissue with long fixation times, and were not found in disease-related tissue fixated for a short period.

The exact mechanism of the described storage related art1facts is not known from previous studies, but formalin solutions are known to become more acidic over time (29). This was confirmed by pH measurements of the excess formalin around our sealed fixed brain tissue. Possibly neuropil destruction is caused by a local increase of acidity. However, continuous exposure to formalin and/or formic acid may form many other compounds that possibly play a role in causing artifactual tissue changes (29, 30). We were not able to study the effect of long term fixation in regularly refreshed formalin, and we can thus not exclude prolonged immersion in formalin itself as a cause of local neuropil destruction leading to MR hypointensities rather than the increasing acidity or the formation of aggressive metabolites. Postmortem autolysis does not appear to be the cause of the artifacts we have observed.

For this study, sufficient material fixed for a period of 1-6 years was lacking. Consequently, we can only conclude that neuropil artefacts occur in all tissue stored for a period of at least 6 years within the same formalin, whereas tissue stored for a period of <1 year showed no changes.

The coarse hypointensities correspond macroscopically to homogeneous white discolourations in the tissue, and microscopically in 8μm HE sections to granular neuropil alterations with slightly less density than the surrounding neuropil. The ultrathin sections (90 nm thick) used for EM re-

vealed that these areas represented absent neuropil with partial filling of the resulting spaces by membrane-like structures. We speculate that this degenerated membranous/proteineous material with weak birefringence causes hypointensities on MRI because of its solid-state-like properties.
The low signal intensity on MRI may also result from replacement of formalin solution by proton free fluid in these relatively more empty spaces. However, a decrease in proton density would not cause a T2* decrease, as was observed in the T2* maps.

With respect to the induced MR changes, previous reports state that formalin fixation causes changes in relaxation and diffusion properties, thereby altering MR contrast, even though the exact mechanism remains unclear (16). However, these changes in MR properties occur throughout the entire sample and are partially reversible by rehydrating the sample in PBS. In contrast, the structural disruptions we found after prolonged formalin fixation are very localized and irreversible. Furthermore, detected changes were not related to any of the known possible changes due to prolonged PMI as described elsewhere (13,15,17,20,21). For this study brain tissue of all kinds of PMI periods was used, and no correlation was found with either the tissue changes or MRI hypointensities (Table 1).

The conclusion of this study suggests that data of several earlier published studies, using postmortem brain tissue of patients with AD for MRI (1-12), should be cautiously interpret. In these studies, hypointense spots were observed on T2* or T2-weighted scans that co-localized with dense amyloid plaques and iron accumulations (1-12). However, brain tissue in these studies was collected within a short period, and fixed for a maximum period of a few months.
With regard to the detection of amyloid plaques, we also observed hypointense spots on MRI that corresponded to the presence of amyloid plaques. However, these did not correlate with the larger stellar shape coarse hypointensities (Fig.4). The possible Aβ plaque detection indicates that the basic mechanisms for MR contrast (iron accumulation and dense protein aggregates) are still present. On ultrahigh resolution scans, these different hypointensities can be easily distinguished. However, on scans with a lower resolution, e.g., those comparable with resolutions that can be achieved on clinical MRI systems, both forms might become indistinguishable, and based on their size the coarse hypointensities because of fixation artifacts are more likely to remain visible (Fig. 1D). In our

study, these low resolution images were acquired at relatively short echo times; when a stronger T2*-weighting would be used, more hypointensities would be observable at these lower resolutions. Furthermore, it is important to realize that although these neuropil changes are beyond the anatomical resolution of scans with clinical resolutions, they could still be visible on such scans because their signal differs so strongly from surrounding tissue.

Other known sources for hypointensities on T2*-weighted images, like calcifications, iron deposits, microbleeds or cavernous malformations (31) could be easily disregarded within this study, whereas their presence could not be confirmed on histology. However, especially when conducting similar ex vivo MR studies for either one of these pathologies using old brain material and clinically relevant resolutions, one should be aware that the described formalin fixation artifacts could possibly lead to similar hypointensities and thus a misinterpretation of the data.

To put our findings into a broader perspective, a small survey was conducted among eight other brain banks and neuropathology departments regarding their brain storage protocol. Three of these centres store their formalin-fixed brain tissue in sealed plastic bags with little excess formalin similar to the tissue used in this study, whereas four other centres store fixed brain tissue floating in formalin, two without a protocol for regularly refreshing it, one renewing formalin "when necessary" and the fourth every few years. The last centre stores brains in polyethyleenglycol. How the different storage protocols affect the general tissue quality with respect to ex vivo MRI research after long term storage remains to be further investigated, but this small survey shows that the fixation protocol for our study is common practice among brain banks, and therefore the findings will have implications for future research on brain bank tissue.

In conclusion, our results demonstrate that fixed brain tissue stored for prolonged periods gives rise to structural tissue changes that are associated with hypo intensities on T2*-weighted MR images. When brain tissue from pathology archives or brain banks is used to study (rare) disorders with ex vivo MRI, it is of vital importance to take the storage protocol into account and to check for the macroscopic and microscopic alterations that have been described and illustrated in this study.

Acknowledgements

Authors want to thank I. Hegeman-Kleinn and C. Welling-Graafland for technical assistance.

Reference List

1. Benveniste H, Einstein G, Kim KR, Hulette C, Johnson GA. Detection of neuritic plaques in Alzheimer's disease by magnetic resonance microscopy. Proc Natl Acad Sci U S A 1999;96(24):14079-14084.

2. Bobinski M, de Leon MJ, Wegiel J, DeSanti S, Convit A, Saint Louis LA, Rusinek H, Wisniewski HM. The histological validation of post mortem magnetic resonance imaging-determined hippocampal volume in Alzheimer's disease. Neuroscience 2000;95(3):721-725.

3. Bronge L, Bogdanovic N, Wahlund LO. Postmortem MRI and histopathology of white matter changes in Alzheimer brains. A quantitative, comparative study. Dement Geriatr Cogn Disord 2002;13(4):205-212.

4. Englund E, Sjobeck M, Brockstedt S, Latt J, Larsson EM. Diffusion tensor MRI post mortem demonstrated cerebral white matter pathology. J Neurol 2004;251(3):350-352.

5. Fernando MS, O'Brien JT, Perry RH, English P, Forster G, McMeekin W, Slade JY, Golkhar A, Matthews FE, Barber R, Kalaria RN, Ince PG. Comparison of the pathology of cerebral white matter with post-mortem magnetic resonance imaging (MRI) in the elderly brain. Neuropathol App Neurobiol 2004;30(4):385-395.

6. Geurts JJ, Bo L, Pouwels PJ, Castelijns JA, Polman CH, Barkhof F. Cortical lesions in multiple sclerosis: combined postmortem MR imaging and histopathology. AJNR Am J Neuroradiol 2005;26(3):572-577.

7. Gouw AA, Seewann A, Vrenken H, van der Flier WM, Rozemuller JM, Barkhof F, Scheltens P, Geurts JJ. Heterogeneity of white matter hypointensities in Alzheimer's disease: post-mortem quantitative MRI and neuropathology. Brain 2008;131(Pt 12):3286-3298.

8. House MJ, St Pierre TG, Kowdley KV, Montine T, Connor J, Beard J, Berger J, Siddaiah N, Shankland E, Jin LW. Correlation of proton transverse relaxation rates (R2) with iron concentrations in postmortem brain tissue from alzheimer's disease patients. Magn Reson Med 2007;57(1):172-180.

9. Kangarlu A, Bourekas EC, Ray-Chaudhury A, Rammohan KW. Cerebral cortical lesions in multiple sclerosis detected by MR imaging at 8 Tesla. AJNR Am J Neuroradiol 2007;28(2):262-266.

10. Larsson EM, Englund E, Sjobeck M, Latt J, Brockstedt S. MRI with diffusion tensor imaging post-mortem at 3.0 T in a patient with frontotemporal dementia. Dement Geriatr Cogn Disord 2004;17(4):316-319.

11. Schmierer K, Parkes HG, So PW, An SF, Brandner S, Ordidge RJ, Yousry TA, Miller DH. High field (9.4 Tesla) magnetic resonance imaging of cortical grey matter lesions in multiple sclerosis. Brain 2010;133(Pt 3):858-867.

12. van Rooden S, Maat-Schieman ML, Nabuurs RJ, van der Weerd L, van Duijn S, van Duinen SG, Natte R, van Buchem MA, van der Grond J. Cerebral amyloidosis: postmortem detection with human 7.0-T MR imaging system. Radiology 2009;253(3):788-796.

13. Blamire AM, Rowe JG, Styles P, McDonald B. Optimising imaging parameters for post mortem MR imaging of the human brain. Acta Radiol 1999;40(6):593-597.

14. Dawe RJ, Bennett DA, Schneider JA, Vasireddi SK, Arfanakis K. Postmortem MRI of human brain hemispheres: T2 relaxation times during formaldehyde fixation. Magn Reson Med 2009;61(4):810-818.

15. Pfefferbaum A, Sullivan EV, Adalsteinsson E, Garrick T, Harper C. Postmortem MR imaging of formalin-fixed human brain. Neuroimage 2004;21(4):1585-1595.

16. Shepherd TM, Thelwall PE, Stanisz GJ, Blackband SJ. Aldehyde fixative solutions alter the water relaxation and diffusion properties of nervous tissue. Magn Reson Med 2009;62(1):26-34.

17. Shepherd TM, Flint JJ, Thelwall PE, Stanisz GJ, Mareci TH, Yachnis AT, Blackband SJ. Postmortem interval alters the water relaxation and diffusion properties of rat nervous tissue--implications for MRI studies of human autopsy samples. Neuroimage 2009;44(3):820-826.

18. Tovi M, Ericsson A. Measurements of T1 and T2 over time in formalin-fixed human whole-brain specimens. Acta Radiol 1992;33(5):400-404.

19. Yong-Hing CJ, Obenaus A, Stryker R, Tong K, Sarty GE. Magnetic resonance imaging and mathematical modeling of progressive formalin fixation of the human brain. Magn Reson Med 2005;54(2):324-332.

20. Nagara H, Inoue T, Koga T, Kitaguchi T, Tateishi J, Goto I. Formalin fixed brains are useful for magnetic resonance imaging (MRI) study. J Neurol Sci 1987;81(1):67-77.

21. D'Arceuil HE, Westmoreland S, de Crespigny AJ. An approach to high resolution diffusion tensor imaging in fixed primate brain. Neuroimage 2007;35(2):553-565.

22. Metz B, Kersten GF, Hoogerhout P, Brugghe HF, Timmermans HA, de JA, Meiring H, ten HJ, Hennink WE, Crommelin DJ, Jiskoot W. Identification of formaldehyde-induced modifications in proteins: reactions with model peptides. J Biol Chem 2004;279(8):6235-6243.

23. Puchtler H, Meloan SN. On the chemistry of formaldehyde fixation and its effects on immunohistochemical reactions. Histochemistry 1985;82(3):201-204.

24. LeVine SM. Oligodendrocytes and myelin sheaths in normal, quaking and shiverer brains are enriched in iron. J Neurosci Res 1991;29(3):413-419.

25. Smith MA, Harris PL, Sayre LM, Perry G. Iron accumulation in Alzheimer disease is a source of redox-generated free radicals. Proc Natl Acad Sci U S A 1997;94(18):9866-9868.

26. Natte R, Maat-Schieman ML, Haan J, Bornebroek M, Roos RA, van Duinen SG. Dementia in hereditary cerebral haemorrhage with amyloidosis-Dutch type is associated with cerebral amyloid angiopathy but is independent of plaques and neurofibrillary tangles. Ann Neurol 2001;50(6):765-772.

27. Viale G, Gambacorta M, Coggi G, Dell'Orto P, Milani M, Doglioni C. Glial fibrillary acidic protein immunoreactivity in normal and diseased human breast. Virchows Arch A Pathol Anat Histopathol 1991;418(4):339-348.

28. Natte R, Yamaguchi H, Maat-Schieman ML, Prins FA, Neeskens P, Roos RA, van Duinen SG. Ultrastructural evidence of early non-fibrillar Abeta42 in the capillary basement membrane of patients with hereditary cerebral haemorrhage with amyloidosis, Dutch type. Acta Neuropathol 1999;98(6):577-582.

29. Matubayasi N, Nakahara M. Hydrothermal reactions of formaldehyde and formic acid: free-energy analysis of equilibrium. J Chem Phys 2005;122(7):074509.

30. Schrag M, Dickson A, Jiffry A, Kirsch D, Vinters HV, Kirsch W. The effect of formalin fixation on the levels of brain transition metals in archived samples. Biometals 2010.(Epub ahead of print)

31. Greenberg SM, Vernooij MW, Cordonnier C, Viswanathan A, Al-Shahi SR, Warach S, Launer LJ, van Buchem MA, Breteler MM. Cerebral microbleeds: a guide to detection and interpretation. Lancet Neurol 2009;8(2):165-174.